PHYSICAL REVIEW E VOLUME 58, NUMBER 1 JULY 1998

$K\beta$ line emission in fusion plasmas

F. B. Rosmej*
Ruhr-Universität Bochum, Institut für Experimentalphysik V, Universitätsstrasse 150, D-44780 Bochum, Germany
(Received 3 March 1998)

Enhanced $K\beta$ line emission ratios from highly charged He-like ions are investigated. Collisional radiative cascades, charge exchange processes, temperature and density variations, and spatial inhomogeneities are considered under typical conditions of fusion plasmas. $K\beta$ Rydberg satellites $1s3lnl'$, which merge into the $K\beta$ lines, are considered. Detailed numerical calculations are carried out for Argon. The present results are in excellent agreement with experimental observations. [S1063-651X(98)50407-2]

PACS number(s): 52.25.Nr, 52.55.Fa, 32.70.Fw

Soft x-ray line emission of highly charged H- and He-like ions is widely used for plasma diagnostics. The $K\beta$ line intensities of He-like ions ($K\beta_1$ is the transition $1s3p\ ^1P_1 \rightarrow 1s^2\ ^1S_0 + h\nu_1$, $K\beta_2$ is the transition $1s3p\ ^3P_1 \rightarrow 1s^2\ ^1S_0 + h\nu_2$) and its adjacent dielectronic satellites $1s2131'$ have been employed for diagnostics in laser produced plasmas, magnetically confined fusion plasmas and inertial confined fusion plasmas [1–4,6].

Recently, high $K\beta$ intensity ratios have been observed in a tokamak being in contradiction to theoretical models [3] by about a factor of 2, although the parameter conditions were well defined. In the present work we consider possible mechanisms leading to enhanced $K\beta$ intensity ratios: charge exchange processes into excited states, collisional radiative cascading contributions, density and temperature effects together with spatial inhomogeneities and overlapping dielectronic Rydberg satellites $1s3lnl'$ with $n=3-6$.

Investigations of cascading contributions have been performed employing a detailed atomic kinetic level system of the He-like ions; see Table I. Full J-splitting for $n=2$ and $n=3$, singlet and triplet splitting, as well as orbital splitting is carried up to $n=9$ for the exact calculation of collisional radiative cascades in low and high density plasmas. All collisional transitions from the ground state and between the excited states are calculated, radiative decay rates are included for $\Delta l=\pm 1$ for $\Delta S=0$, 1 for all transitions up to $n=9$ in addition to other relevant ones (e.g., two photon transitions and electric/magnetic multipole transitions from the $1s2s\ ^1S_0$, $1s2s\ ^3S_1$, and $1s2p\ ^3P_2$ levels). Calculations are carried out with the MARIA code [5], and further details and applications are described elsewhere [7,8].

Figure 1 shows the $K\beta_2$ to $K\beta_1$ line intensity ratio as a function of the electron temperature for various electron densities. Due to the different high energy asymptotes of the radial direct ($\sigma_d^{(r)}$) and exchange ($\sigma_e^{(r)}$) part of the excitation cross sections

$$\sigma_d^{(r)}(K\beta_1) \propto \ln E/E, \quad \sigma_e^{(r)}(K\beta_2) \propto 1/E^3, \tag{1}$$

the $K\beta_2/K\beta_1$ intensity ratio falls off with increasing temperature. Equations (1) are strictly valid only in LS coupling. In intermediate coupling, the cross sections for the excitation of the He-like $1snl$ levels from the ground state $1s^2\ ^1S_0$ can be written [9]

$$\sigma = Q_d\sigma_d^{(r)} + Q_e\sigma_e^{(r)}. \tag{2}$$

Q_d and Q_e are the angular factors. For argon, intermediate coupling with inclusion of relativistic effects [9,10] give a value for the direct (Q_d) and exchange (Q_e) angular part of 0.9818/0.25 respectively for the $K\beta_1$ excitation and 1.821×10^{-2}/0.25 for the $K\beta_2$ excitation. Intermediate coupling effects are therefore small. With increasing density, the ratio rises because effective collisional transfer of population from the $1s3s\ ^3S_1$, $1s3p\ ^3P_{0,2}$, and $1s3d\ ^3D_{1,2,3}$ levels to the $1s3p\ ^3P_1$ takes place (note that the population transfer inside the $1s3l$-level structure is treated with inclusion of all monopole, dipole and quadrupole transitions taking into account intermediate coupling and relativistic effects).

The influence of charge exchange processes and subsequent collisional radiative cascades on the $K\beta$ lines requires not only the consideration of the processes

$$H + Ar^{17+} \rightarrow H^+ + Ar^{17+}(1snl),$$

but also the charge exchange processes to all ionization stages too, to account for the proper ionization balance shift. Because charge exchange couples into the excited states $1snl$, numerous collisional radiative cascades are initiated:

$$Ar^{17+}(1snl) \rightarrow \left\{ \begin{array}{c} 1s^2 + h\nu_{n1} \\ 1s2l + h\nu_{n2} \\ 1s3l + h\nu_{n3} \\ \cdots \end{array} \right\} \rightarrow \left\{ \begin{array}{c} 1s^2 + h\nu_{21} \\ 1s^2, 1s2l + h\nu_{32} \\ \cdots \end{array} \right\} \rightarrow \left\{ \begin{array}{c} -, 1s^2 + h\nu_{21} \\ \cdots \end{array} \right\}.$$

For argon $n \approx 8$ and the main population transfer through cascading takes place to the $1s2l$ and $1s3l$ levels. A minor transfer takes place into other channels (due to low radiative decay rates and branching ratios). Cascading population transfer to the $1s2l$ levels leads to a rise of the $x = 1s^2 - 1s2p\ ^3P_2$, $y = 1s^2 - 1s2p\ ^3P_1$, $z = 1s^2 - 1s2s\ ^3S_1$ emission lines ($K\alpha$ lines) and the ionization balance shift raises

*Electronic address: frank.b.rosmej@ruhr-uni-bochum.de

TABLE I. He-like levels included in the kinetic modeling for the exact consideration of collisional radiative cascade contribution to the $K\beta$ emission lines.

Ion	Configurations
He-like	$1s^2\ ^1S_0, 1s2s\ ^1S_0, 1s2s\ ^3S_1, 1s2p\ ^1P_1, 1s2p\ ^3P_0, 1s2p\ ^3P_1, 1s2p\ ^3P_2, 1s3s\ ^1S_0,$ $1s3d\ ^3S_1, 1s3p\ ^1P_1, 1s3p\ ^3P_0, 1s3p\ ^3P_1, 1s3p\ ^3P_2, 1s3d\ ^1D_2, 1s3d\ ^3D_1, 1s3d$ $^3D_2, 1s3d\ ^3D_3, 1s4s\ ^1S, 1s4s\ ^3S, 1s4p\ ^1P, 1s4p\ ^3P, 1s4d\ ^1D, 1s4d\ ^3D, 1s4f$ $^1F, 1s4f\ ^3F, 1s5s\ ^1S, 1s5s\ ^3S, 1s5p\ ^1P, 1s5p\ ^3P, 1s5d\ ^1D, 1s5d\ ^3D, 1s5f\ ^1F,$ $1s5f\ ^3F, 1s5g\ ^1G, 1s5g\ ^3G, 1s6s\ ^1S, 1s6s\ ^3S, 1s6p\ ^1P, 1s6p\ ^3P, 1s6d\ ^1D,$ $1s6d\ ^3D, 1s6f\ ^1F, 1s6f\ ^3F, 1s6g\ ^1G, 1s6g\ ^3G, 1s6h\ ^1H, 1s6h\ ^3H, 1s7s\ ^1S,$ $1s7s\ ^3S, 1s7p\ ^1P, 1s7p\ ^3P, 1s7d\ ^1D, 1s7d\ ^3D, 1s7f\ ^1F, 1s7f\ ^3F, 1s7g\ ^1G, 1s7g$ $^3G, 1s7h\ ^1H, 1s7h\ ^3H, 1s7i\ ^1I, 1s7i\ ^3I, 1s8s\ ^1S, 1s8s\ ^3S, 1s8p\ ^1P, 1s8p\ ^3P,$ $1s8d\ ^1D, 1s8d\ ^3D, 1s8f\ ^1F, 1s8f\ ^3F, 1s8g\ ^1G, 1s8g\ ^3G, 1s8h\ ^1H, 1s8h\ ^3H,$ $1s8i\ ^1I, 1s8i\ ^3I, 1s8k\ ^1K, 1s8k\ ^3K, 1s9s\ ^1S, 1s9s\ ^3S, 1s9p\ ^1P, 1s9p\ ^3P, 1s9d$ $^1D, 1s9d\ ^3D, 1s9f\ ^1F, 1s9f\ ^3F, 1s9g\ ^1G, 1s9g\ ^3G, 1s9h\ ^1H, 1s9h\ ^3H, 1s9i\ ^1I,$ $1s9i\ ^3I, 1s9k\ ^1K, 1s9k\ ^3K, 1s9l\ ^1L, 1s9l\ ^3L$

the inner-shell excited Li-like $n=2$ satellites $1s2l2l'$ [11]. Figure 2 shows the $K\beta$ ratio in dependence of various neutral beam fractions $f=n_{\text{neutral}}/n_e$, n_{neutral} is the neutral hydrogen density, $n_e=10^{14}$ cm^{-3}, $kT_i=1.5$ keV (corresponding to a neutral background), $A=1.8$ (number of nucleons for a mixture of hydrogen and deuterium) are held fixed. For relative neutral fractions larger than 10^{-6} and temperatures kT_e above 1.5 keV charge exchange influences visibly the $K\beta$ line emission. For lower temperatures the cascading contributions decrease due to the low population of the H-like ground state $1s\,^2S_{1/2}$.

Figure 3 shows the $K\beta$-Rydberg satellites of the type $1s3lnl' \rightarrow 1s3lnl''+h\nu$ with $n=3-6$ (and all orbital momenta $1=s,p,d,f,g,h$) which merge into the $K\beta$ lines. Atomic data for these satellites have been calculated with the Hartree-Fock method HFR [12] including extended configuration interaction and relativistic effects up to the second order. The dashed line shows the emission without dielectronic satellites, and the solid line includes all these satellites. For the parameters chosen ($kT_e=500$ eV, $n_e=10^{19}$ cm^{-3}) these satellites effectively contribute mainly to the red wing of the $K\beta$ structure, and, hence, do not significantly increase the $K\beta$-line intensity ratio.

Table II compares the present theoretical calculations for $kT_e=2.3$ keV, $n_e=1.5\times10^{13}$ cm^{-3} and the experimental high precision measurements of Beiersdorfer *et al.* at the Princeton Tokamak [3]. Due to the high central temperature the intensity from dielectronic satellites $1s3lnl'$ is negligible (this might not be the case in, e.g., laser produced plasmas with relatively cold and dense target plasmas). The first column has been calculated for a single temperature only (the central electron temperature), giving a ratio of 0.043. The second column takes into account the spatial variation of the electron temperature and the electron density across the minor radius (parabolic dependence), giving a ratio of 0.048. The rise of the $K\beta$ ratio in inhomogeneous plasmas is caused by the relative rise of the exchange part of the collisional cross sections; see Fig. 1 and Eq. (1). The present theoretical calculations are therefore in excellent agreement with the measurements, whereas [3] obtained large theoretical discrepancies.

Let us consider a simplified analytic model for the $K\beta$ emission at low densities to clarify the importance of various population channels: electron collisional excitation from the He-like ground state $1s^2\,^1S_0$, charge exchange and radiative recombination from the H-like ground state $1s\,^2S_{1/2}$ into the $1s3p\,^1P_1$ and $1s3p\,^3P_1$ levels via direct and cascading processes,

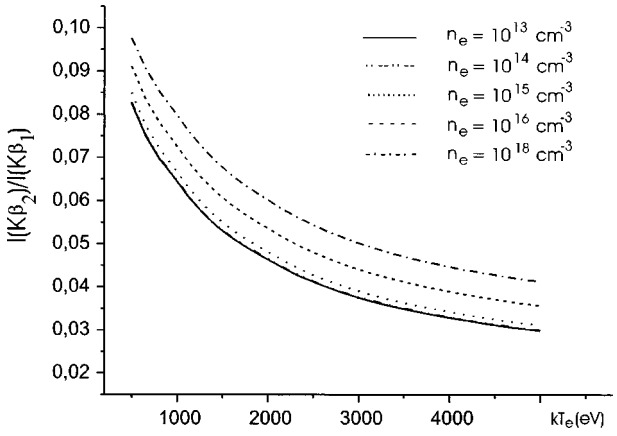

FIG. 1. Intensity ratio of the $K\beta_2$ and $K\beta_2$ lines in dependence of the electron temperature for various electron densities n_e.

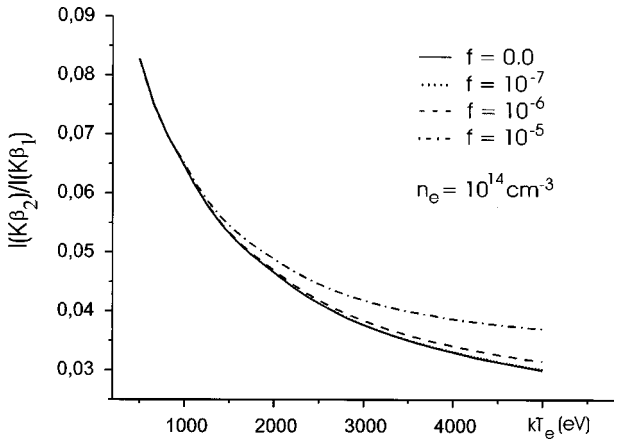

FIG. 2. Intensity ratio of the $K\beta_2$ and $K\beta_1$ lines in dependence of the electron temperature showing the influence of charge exchange processes (background of neutrals; see text) through collisional radiative cascades for various fractions of neutrals f, $n_e=10^{14}$ cm^{-3}.

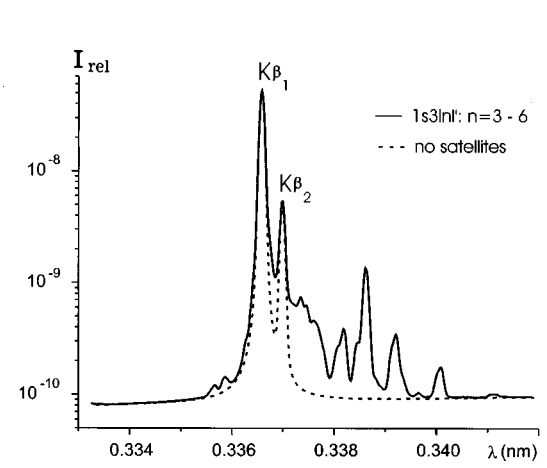

FIG. 3. Line overlapping of dielectronic Rydberg satellites $1s3lnl'$ with the $K\beta$ lines, $n_e=10^{19}$ cm^{-3}, $kT_e=500$ eV.

$$I\beta_1 \approx \frac{A_1}{A_1+\sum_{A\neq A_1} A(^1L)} \left\{ n_e n(1s) R\beta_1 + n_e n(1s^2) C\beta_1 + n_H n(1s) \sum_n b_1(n) C x_1(nd) \right\}, \tag{3}$$

$$I\beta_2 \approx \frac{A_2}{A_2+\sum_{A\neq A_2} A(^3L)} \left\{ n_e n(1s) R\beta_2 + n_e n(1s^2) C\beta_2 + n_H n(1s) \sum_n b_1(n) C x_2(nd) \right\}, \tag{4}$$

with

$$R\beta_1 = R_1(3\ ^1P_1) + b_1(4) R(4\ ^1D_2) + \cdots,$$

$$R\beta_2 = R_2(3\ ^3P_1) + b_2(4) R(4\ ^3D) + \cdots, \tag{5a}$$

$$C\beta_1 = C_1(3\ ^1P_1) + b_1(4) C(4\ ^1D_2) + \cdots,$$

$$C\beta_2 = C_2(3\ ^3P_1) + b_2(4) C(4\ ^3D) + \cdots \tag{5b}$$

R are the radiative recombination rates, C the electron collisional excitation rates, Cx the charge exchange rates into the $1snd\ ^{1,3}D$ states, and b the branching factors accounting for the different radiative channels. The factor in front of the brackets of Eqs. (3) and (4) take into account the branching ratio (radiative decay to lower excited levels); the most dominating ones are the transitions $1s3p\ ^3P_1 \rightarrow 1s2s\ ^3S_1 + h\nu$ and $1s3p\ ^1P_1 \rightarrow 1s2s\ ^1S_0 + h\nu$. Table III depicts these radiative decay rates (A_1 and A_2 have been calculated with the MZ code, others with the HFR method). By comparing the sums with the respective radiative decay rates A_1 and A_2 into the He-like ground state it turns out that the branching ratio for the triplet system is very important, giving a total branching ratio of only 0.228, whereas the branching ratio in the singlet system is close to 1 (0.942) due to the high radiative decay rate A_1. Retaining only the direct terms populating the upper $1s3p\ ^3P_1$ and $1s3p\ ^1P_1$ levels the $K\beta$ ratio is given by

TABLE II. $K\beta$ intensity ratios: comparisons between the present theoretical calculations and the experimental measurements of Beiersdorfer *et al.* [3]. Taking into account the experimental electron temperature and electron density in the plasma center, $kT_e(r=0)=2.3$ keV, $n_e(r=0)=1.5\times10^{13}$ cm^{-3}, temperature and density inhomogeneities (second column), and full calculation of collision radiative cascades (see Table I), the agreement between the experiment and the present calculations (carried out with the MARIA code) is excellent.

$\frac{I\beta_2(r=0)}{I\beta_1(r=0)}$	$\frac{\int_{r=0}^{a} I\beta_2(r)dr}{\int_{r=0}^{a} I\beta_1(r)dr}$	Experimental ratio
0.043	0.048	0.048±0.003

$$\frac{I\beta_2}{I\beta_1} \approx \frac{A_2}{A1} \frac{A_1+\sum_{A\neq A_1} A(^1L)}{A_2+\sum_{A\neq A_2} A(^3L)} \frac{C_2+r\cdot R_2}{C_1+r\cdot R_1}, \quad r=\frac{n(1s)}{n(1s^2)}. \tag{6}$$

Taking into account the radiative values from Table III and the respective collisional cross sections (calculated with the ATOM code [13] with the Coulomb-Born-exchange method including intermediate coupling and relativistic effects) for $kT_e=2.3$ keV ($r\approx1.3$) this analytic formula delivers a ratio of 0.038. Calculation with the MARIA code with inclusion of the full collisional radiative cascading gives 0.043, without cascading (switching off all the $1s4l$, $1s5l$, $1s6l$, $1s7l$, $1s8l$, and $1s9l$ levels) the ratio is 0.041. This demonstrates that the main processes are depicted by the analytic formula from Eqs. (6). The proposal of [3] that cascading may seriously influence the $K\beta$ emission therefore cannot be confirmed.

The electron collisional rates of [14] for the transitions $1s^2+e \rightarrow 1s3l\ ^{1,3}L+e$ result in decreased $K\beta$ intensity ratios in particular for low temperatures due to the strong contribution of resonance effects. The intensity ratios in Table II, however, change only by about 0.001. We note that [15] stated that the resonance contributions for the $1s^2+e-1s3l\ ^3L+e$ collisional transitions are overestimated by Keenan, McCann, and Kingston [14] and that Coulomb-Born exchange cross sections may be a better choice at present.

The origin of enhanced $K\beta$ intensity ratios is therefore manifold: (i) cascading contributions from high states $1snl\ ^3L$; (ii) charge exchange processes into excited states $1snl$; (iii) density enhanced population of the $1s3p\ ^3P_1$

TABLE III. Radiative decay values and selected branching ratios used in the analytical model for the $K\beta$ ratio, $A_1 = A(1s3p\ ^1P_1 - 1s^2\ ^1S_0)$, $A_2 = A(1s3p\ ^3P_1 - 1s^2\ ^1S_0)$.

A_1(s^{-1})	$\sum_{A\neq A_1} A(^1L)$(s^{-1})	A_2(s^{-1})	$\sum_{A\neq A_2} A(^3L)$ (s^{-1})
2.98×10^{13}	1.86×10^{12}	5.52×10^{11}	1.87×10^{12}

level; (iv) spatial inhomogeneities raising the $K\beta_2$ emission (relative to the $K\beta_1$ emission) through the rise of the exchange part of the collisional cross section for lower temperatures. At low densities, the leading terms for the $K\beta$ ratio are given by Eq. (6).

In conclusion, we have performed a detailed analysis of the $K\beta$ emission lines and their adjacent Rydberg satellites $1s3lnl'$ for diagnostics. Charge exchange processes, temperature and density variations, and spatial inhomogeneities are considered, together with extensive collisional radiative cascades. The present theoretical calculations are in excellent agreement with high precision measurements and recently found discrepancies in the $K\beta$ ratios [3] are not encountered. The $K\beta$ line emissions (intensity ratios) together with the present theoretical modeling can therefore be considered as reliable diagnostics.

[1] V. A. Boiko, A. Ya. Faenov, S. A. Pikuz, I. Yu. Skobelev, A. V. Vinogradov, and E. A. Yukov, J. Phys. B **10**, 3387 (1977).

[2] V. A. Boiko, S. A. Pikuz, U. I. Safranova, and A. Ya. Faenov, Mon. Not. R. Astron. Soc. **185**, 789 (1978).

[3] P. Beiersdorfer, A. L. Osterheld, T. W. Phillips, M. Bitter, K. W. Hill, and S. von Goeler, Phys. Rev. E **52**, 1980 (1995).

[4] N. C. Woolsey, A. Asfaw, B. Hammel, C. Keane, C. A. Back, A. Calisti, C. Mossé, R. Stamm, B. Talin, J. S. Wark, R. W. Lee, and L. Klein, Phys. Rev. E **53**, 6396 (1996).

[5] F. B. Rosmej and J. Abdallah, Jr., Phys. Lett. A (to be published).

[6] F. B. Rosmej, Lett. J. Phys. B.: At. Mol. Opt. Phys. **30**, L819 (1997).

[7] F. B. Rosmej *et al.*, J. Quant. Spectrosc. Radiat. Transf. **58**, 859 (1997).

[8] F. B. Rosmej and *et al.*, JETP Lett. **65**, 708 (1997).

[9] V. P. Shevelko and L. A. Vainshtein, *Atomic Physics for Hot Plasmas* (IOP Publishing, Bristol, 1993).

[10] L. A. Vainshtein and U. I. Safronova, Phys. Scr. **31**, 519 (1985).

[11] F. B. Rosmej and V. S. Lisitsa, Phys. Lett. A (to be published).

[12] R. D. Cowan, *Theory of Atomic Structure and Spectra* (University Press, Berkeley, 1981).

[13] L. A. Vainshtein and V. P. Shevelko (unpublished).

[14] F. P. Keenan, S. M. McCann, and A. E. Kingston, Phys. Scr. **35**, 432 (1987).

[15] S. Nakazaki, K. Sakimoto, and Y. Itikawa, Phys. Scr. **47**, 359 (1993).